Journal of Materials Chemistry B

RSC Publishing

COMMUNICATION

View Article Online
View Journal | View Issue

Shape memory poly(ε-caprolactone)-*co*-poly(ethylene glycol) foams with body temperature triggering and two-way actuation†

Cite this: *J. Mater. Chem. B*, 2013, **1**, 4916

Received 6th June 2013
Accepted 19th August 2013

DOI: 10.1039/c3tb20810a

www.rsc.org/MaterialsB

Richard M. Baker, James H. Henderson and Patrick T. Mather*

We describe the fabrication of porous foams with shape memory triggering at body temperature. Employing a modified porogen-leaching technique, functionalized poly(ε-caprolactone) (PCL) and poly(ethylene glycol) (PEG) macromers are crosslinked *via* thiol–ene chemistry to generate highly porous foam scaffolds with shape memory capacity. The temperature at which shape change of these scaffolds occurs under hydrated conditions can be tuned both through control of the chemical composition and through deformation temperature during mechanical programming of the scaffolds. Uniquely, the foams exhibit reversible actuation in compression, which has not previously been demonstrated for foams. Our results indicate that PCL–PEG shape memory foams have potential as programmable scaffolds for tissue engineering, regenerative medicine, and the study of cell mechanobiology.

There has been significant interest and effort to develop programmable scaffolds capable of dynamically changing shape, porosity, and architecture for application in tissue engineering and regenerative medicine.[1,2] Shape changing scaffolds capable of undergoing large volumetric expansions show promise for minimally invasive delivery, medical applications requiring space-filling constructs, and preparation of tissue engineered constructs for improved cell seeding.[3,4] Scaffolds with dynamic programmability are also anticipated to become powerful tools for the study of cell mechanobiology, providing new understanding of how cells respond to biophysical stimuli. For example, scaffolds that better mimic the dynamic nature of *in vivo* microenvironments, such as extracellular reorganization, could provide new insights for studies of tissue development and disease progression.[5,6]

One approach to develop scaffolds with dynamic programmability is the use of shape memory polymers (SMPs). SMPs are a class of smart materials capable of undergoing a programmed change in shape upon application of an external stimulus, such as heat. Recent studies have employed SMPs as shape changing substrates to investigate cell response to actively changing topographies in 2D.[5,7,8] In the first report of body temperature triggered topography change with attached and viable cells, we found that cells exhibited a change in alignment and morphology due to the dynamic topography change.[5] SMP substrates are expected to be useful platforms to control cell mechanobiological responses in tissue engineering strategies, such as cell sheet engineering, and to study how topographic changes influence cell mechanobiological behaviours such as migration, differentiation, and proliferation.

Moving beyond this work in 2D to scaffolds with 3D structure, Lendlein and colleagues reported an SMP scaffold with programmed pore morphology change at body temperature.[9] Subsequently, we reported the first 3D SMP scaffold with attached and viable cells under body temperature triggering.[10] Cells seeded on an aligned fiber mat showed preferential alignment parallel to the aligned fibers. Upon triggering fiber reorganization to a random orientation, cells reoriented and lost preferential alignment. This recent advancement, accomplished in thin fiber mats, suggests the potential for further advancements in active 3D scaffolds for tissue engineering, regenerative medicine, and study of cell mechanobiology. However, improved control over scaffold porosity and recovery temperature, while maintaining shape memory functionality, is required.

We aimed to address these requirements by developing highly porous SMP scaffolds capable of changing pore size and morphology under body temperature triggering. Here, we show the fabrication and characterization of poly(ε-caprolactone)-*co*-poly(ethylene glycol) (PCL-*co*-PEG) foams with excellent shape memory behavior. Control over the recovery temperature is achieved through scaffold composition and programming conditions.

Syracuse Biomaterials Institute, The Department of Biomedical and Chemical Engineering, Syracuse University, Syracuse, New York, USA. E-mail: ptmather@syr.edu; Tel: +1-315-443-8760

† Electronic supplementary information (ESI) available. See DOI: 10.1039/c3tb20810a

To prepare highly porous scaffolds we used end-linking of telechelic macromers with thiol–ene chemistry,[11,12] combined with a modified porogen-leaching process, similar to a method established by Zhang and colleagues for PCL-*block*-polydimethylsiloxane SMP foams.[13] Functionalized PCL and PEG macromers were dissolved in dichloromethane (DCM) and combined with tetrathiol crosslinker and 2,2-dimethoxy-2-phenylacetophenone photoinitiator (Scheme 1; detailed methods for functionalization and synthesis are provided in the ESI†). This solution was added to fused NaCl crystals in a 1 : 9 polymer–salt ratio by weight and UV cured. The fusion of salt particles, prior to the addition of the macromer solution, was performed to improve the pore interconnectivity.[14] Following curing, salt was extracted in water, yielding highly interconnected porous foams with porosities of 79 ± 5% as determined by microtomography (ESI†).

Shape memory behavior was characterized using a one-way shape memory compression test (Fig. 1a). Prior to testing, samples were thermally treated by heating to 80 °C for 10 min followed by cooling to −4 °C for 10 min to remove residual stresses generated during curing. To test shape memory behavior, circular disks of the scaffold were heated to 80 °C and uniaxially compressed. While maintaining the compressive deformation, the samples were cooled to 0 °C to induce crystallization, immobilizing the chains and fixing the deformation. Upon unloading, a fixing ratio—how much of the programmed deformation is maintained upon unloading—of 99 ± 0.5% was observed. Samples were then heated to 80 °C to trigger recovery of the scaffold, with a recovery ratio—how much of the programmed deformation is recovered upon heating—of 97 ± 1.4% observed. The programmed state remained stable at room temperature with no observable premature recovery during 6 days of storage. Stability of temporary shapes is a desirable characteristic both for tissue engineering scaffolds and for active cell mechanobiology studies, in which cell seeding is performed in the temporary state.

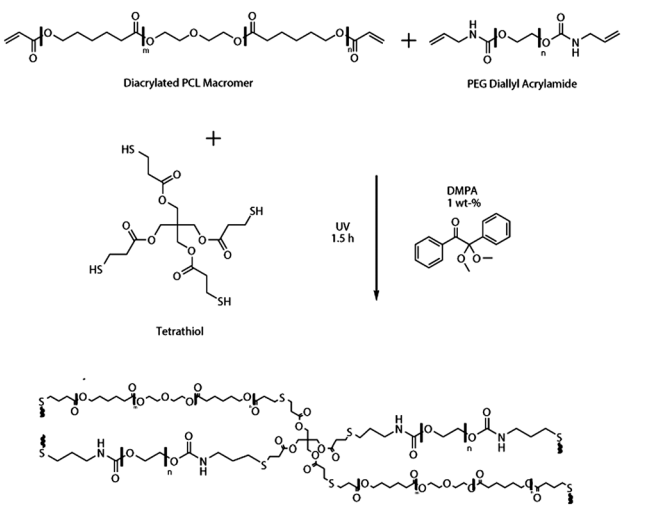

Scheme 1 SMP network formation using photo-initiated addition reactions between oligomeric macromers and the shown tetrathiol.

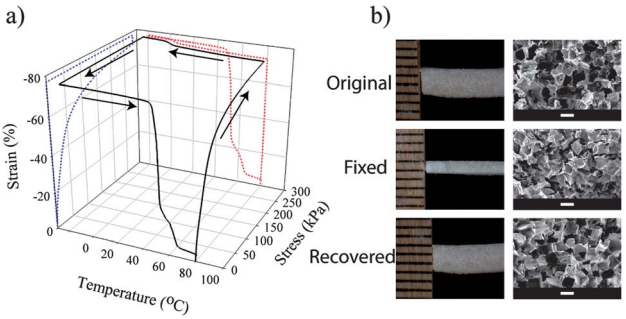

Fig. 1 Shape memory behavior of SMP scaffolds. (a) One-way shape memory cycle of 80PCL–20PEG in compression reveals excellent shape fixing and recovery; (b) optical micrographs (left) and SEM images (right) of scaffold cross-sections prior to compressing 50% (top), after compressing 50% (middle), and after triggering recovery (bottom) reveals porous architecture collapses upon fixing but is subsequently restored following shape recovery. Note that in (a) samples were fixed with 78% compression but in (b) were fixed with only 50% compression to allow SEM visualization of the effect of shape fixing on pore structure without pores being in a completely collapsed state.

To determine the effect of shape memory on macroscopic and microscopic scaffold architecture, scanning electron microscopy (SEM) was performed. Prior to programming the temporary shape, SEM of the scaffold cross-section revealed an open pore structure with high interconnectivity (Fig. 1b). Upon programming the compressive deformation, the porous architecture collapsed as internal walls began layering on top of one another, significantly reducing the porosity. The effect of compressive shape memory on SMP foams has been previously reported by Sauter and colleagues, who reported microscale buckling of struts for foams with monomodal pore distribution, whereas foams with bimodal pore distributions had microscale bending rather than buckling.[15] Importantly, the porous architecture was restored upon recovery of the scaffold, with no obvious compromise of the integrity of the internal foam walls, as observed visually from SEM or mechanically from repeated shape memory cycles where the material's modulus did not drop after three repeated cycles. Large compression ratios of up to 78% (Fig. 2a) were achieved, which is desirable for tissue engineering strategies, such as minimally invasive delivery, or mechanobiological study of large tensile strains on cells seeded in fixed scaffolds. For example, in adult cardiac fibroblasts it has been shown that a 10% uniaxial tensile strain can stimulate extracellular matrix mRNA levels and transform growth factor-β (TGF-β), whereas a 20% strain decreases extracellular matrix mRNA expression while stimulating TGF-β to a lesser extent.[16] Low porosity in the fixed state may inhibit cell infiltration into the scaffold when seeding in the temporary state. As a result, tissue engineering applications or cell mechanobiology studies for which large strain triggering is desired necessitate balancing of the desired strain with the ability to achieve cell seeding in the fixed, low porosity state. Therefore, to enable studies on increasing levels of strain recovery, increasing porosity in the permanent state will be required. SMP scaffolds fabricated *via* the alternative method of gas foaming have been developed with permanent porosities of 98%,[17] but with gas foaming pore interconnectivity is typically low,[18] which would limit cell

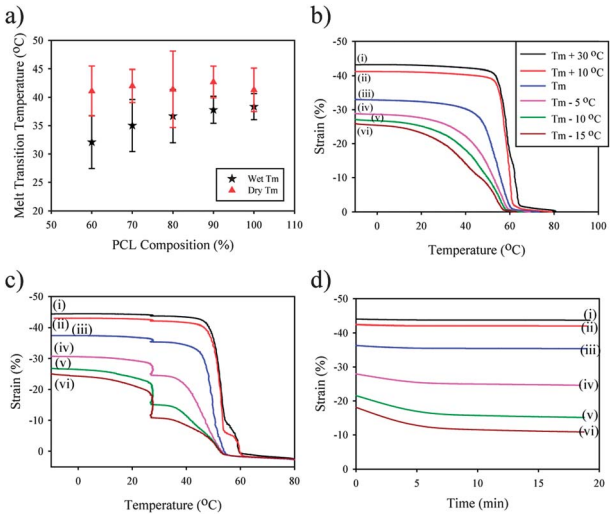

Fig. 2 Controlling recovery temperature of SMP scaffolds. (a) Melting transition temperatures measured from DSC decrease with increasing PEG wt% in both the dry and hydrated states. (b) Deforming at lower temperatures leads to an earlier onset temperature of recovery. Fixed samples were heated at 3 °C min^{-1} to 80 °C. (c) Deforming at lower temperatures leads to a decrease in stability near room temperature. Fixed samples were heated at 3 °C min^{-1} to 27 °C and held isothermal for 20 min to observe stability, followed by heating at 3 °C min^{-1} to 80 °C for full recovery. (d) Stability of the fixed shape during the isothermal step at 27 °C is reduced. For (b–d) deformation temperatures are: (i) T_m + 30, (ii) T_m + 10, (iii) T_m, (iv) T_m − 5, (v) T_m − 10, (vi) T_m − 15. A composition of 80PCL–20PEG was used for the temperature deformation studies.

infiltration into such scaffolds. For the salt leaching approach employed in the present work, pore size, porosity and interconnectivity can be tuned by control over salt particle size, degree of salt fusion, and macromer concentration.[13] Control over the porous structure is important for cell mechanobiology studies, as previous studies on static scaffolds have shown that cell behavior is dependent on pore morphology and size.[19,20]

Shape-changing scaffolds that can change shape under cell compatible conditions, particularly at or near body temperature, require control over the triggering mechanism. Shape recovery of semi-crystalline SMPs occurs at their melting transition temperature (T_m), and the T_m of PCL is ~60 °C, which is much higher than body temperature. Therefore, lowering of T_m is necessary to fabricate a shape-changing PCL-based construct. Here we have achieved lowering of T_m *via* two mechanisms. The first mechanism utilized copolymerization of macromers of PCL with PEG, a hydrophilic polymer. We previously reported a PCL–PEG hydrogel with a T_m of 31 °C, where tuning of the T_m was achieved through control over the molecular weight of the PCL.[21] Here we kept the molecular weight of the macromers constant and varied the weight ratios of each to control the T_m. Differential scanning calorimetry (DSC) revealed that the T_m of the scaffold in both the dry and wet states decreased with increasing PEG content (Fig. 2a). DSC traces of films revealed a similar trend (ESI; Fig. S4†) supporting the notion of a primarily compositional effect. As a consequence of increasing PEG, the water uptake of foams also increased (ESI; Fig. S8†). Employing this design strategy, a range of T_ms around body temperature was achieved, with a composition of 80 wt% PCL and 20 wt% PEG yielding a hydrated T_m of 37 °C.

In addition to copolymerizing the PCL scaffolds with PEG for melting point modulation, we also varied the programming temperature of the SMP foam to lower the apparent T_m, or onset temperature for shape recovery. Scaffolds with a composition of 80PCL–20PEG were heated to different temperatures ranging from 25 °C to 70 °C then uniaxially compressed. After reaching either a predetermined strain of 30% or the force limit of the tensile testing device, the scaffolds were next cooled to −10 °C to fix the deformation by crystallization. Following unloading, scaffolds were heated at 3 °C min^{-1} to 80 °C to observe recovery. The compressive strains fixed (observed as the starting strains in Fig. 2b) varied with the deformation temperature (ESI; Fig. S5†). Samples compressed above T_m before cooling experience a spontaneous additional strain during crystallization (described further in Fig. 3), while those deformed below Tm did not. Further, strains fixed by deforming at or below T_m did so with a different mechanism than the conventional shape memory effect; specifically plastic deformation of the crystalline phase that is recoverable upon subsequent heating through T_m.[22,23]

Apparent from Fig. 2b is the fact that strains fixed by this mechanism decrease with decreasing temperature. Concerning the strain recovery profiles, it was observed that for deformations well above T_m of the construct, there was little dependence of recovery onset temperature on deformation temperature (Fig. 2b). However, as the deformation temperature approached T_m from above, an associated decrease in the onset temperature was observed. One-way shape memory testing of foams deformed at 80 °C to different strains (and thus densities) revealed this was not an effect of heat transfer differences (ESI; Fig. S6†), but rather an effect of the deformation temperature. A similar "temperature memory" phenomenon has previously been reported by Xie *et al.* for a Nafion-based SMP, where a large alpha transition related to the ionic cluster phase is largely responsible for this effect.[24] A related phenomenon has been exploited in amorphous systems to tune the recovery temperature and recovery kinetics,[9,25] where deforming at or below the glass transition temperature led to lower recovery temperatures. Kratz and colleagues also reported this phenomenon in semi-crystalline polymers with a broad T_m where recovery

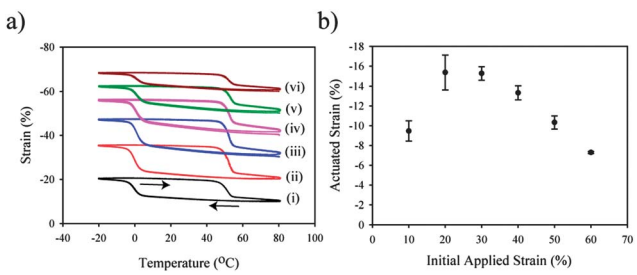

Fig. 3 Two-way reversible actuation. (a) An 80PCL–20PEG SMP foam showed reversible two-way actuation of up to 15% when a constant load is applied during crystallization ((i) 10%, (ii) 20%, (iii) 30%, (iv) 40%, (v) 50%, and (vi) 60% initial applied strain); (b) a maximum actuation strain is observed with a prestrain of 30%, and the actuation strain decreases as the prestrain deviates from 30%.

temperatures spanning a range of 100 °C were achieved.[26] In contrast, the present temperature memory is not attributed to a broad T_m, but rather to apparently lower thermal energy required to recover the plastic deformation of the crystalline phase in comparison to the deformed-then-crystallized case. The present work is the first report of semi-crystalline SMP foams exhibiting a temperature memory effect.

Although deforming near T_m results in a lowering of the onset temperature for strain recovery to within a physiological range, an unintended consequence of this approach is a reduction in the stability of the temporary shape at room temperature. This was examined by dwelling at that temperature during the heating step of the shape memory cycle (Fig. 2c and d). We attribute the reduction in fixed strain stability at room temperature to relaxation of internal stresses between the high melting fraction of the material, which is elastically deformed at the lower temperature and thus under compressive stress, and the lower melting fraction that is subject to tensile stress from the high-melting fraction. Despite these complexities, the temperature memory effect offers a useful tool to control the recovery temperature of this SMP foam. Used in combination with composition-variation to tune equilibrium T_m, this approach will yield adequate design flexibility for biological experiments, we anticipate.

Surprisingly, the new shape memory foams also exhibited two-way reversible shape memory (Fig. 3) under the bias of a compressive load, consisting of dramatic cooling-induced compression and heating-induced expansion. By inspection, neither effect is due to ordinary thermal expansion effects; rather, crystallization of the foams under a compressive load results in additional contraction that is reversed upon heating through T_m, with thermal hysteresis of *ca.* 50 °C when a heating rate of 3 °C min^{-1} is used. This effect is repeatable through several cool–heat cycles and represents a new example of reversible, soft actuation. For these samples, a compressive actuation strain of *ca.* 15% (Fig. 3b) was achieved through contraction upon crystallization. Interestingly, the actuation magnitude (strain) was found to be non-monotonic in the initial strain applied, indicating competing effects of strain that drives crystallization-induced actuation, and an upper bound of compressive strain for the foams. The observed compressive two-way shape memory is not explicitly due to the material's porous structure, as solid cylinders of the material in compression also were found to exhibit a similar effect (ESI; Fig. S7†). However the actuation strain achieved with the porous structure is much larger than that achieved in the solid, non-porous structure, a finding likely related to the complex distribution of stress within compressed open-cell foams.[27] We have previously reported two-way shape memory in a cross-linked poly(cyclooctene) film under tensile loading.[28] Other studies have also reported the use of the two-way shape memory effect in shape memory elastomers,[29] glass-forming nematic networks,[30] and triple-shape SMPs,[31] all of which use tensile loading. To our knowledge, this is the first demonstration of an SMP scaffold with two-way reversible shape memory in compression. Two-way reversible actuation has been studied in other material systems, such as shape memory alloys, for application in reversible actuators.[32] Incorporating this functionality in a cytocompatible scaffold creates the possibility for generating cyclic loading on attached cells by simply switching the incubation temperature. This would enable studies into the effects of low frequency cyclic loading on cell behavior without the need of complex bioreactors or specialized loading devices. Further optimization is needed to decrease the thermal hysteresis of actuation, affording cytocompatiblity for both compression and expansion.

The new PCL-*co*-PEG foam reported here shows promise as a tool for studying cell mechanobiology in 3D, and potential to enable minimally invasive delivery of scaffold constructs. As a scaffold, the foams could enable filling of critical-size bone defects. SMPs have also previously been proposed for deployable medical devices including aneurysm occlusion devices,[33–35] ischemic stroke devices,[36] and stents.[25,37] For minimally invasive delivery in any of these applications, SMP scaffolds must have high compression ratios with high stability of the fixed shape. The foam presented here exhibited a high compression ratio of 78% and was able to recover 97% of the programmed deformation. Recovery at body temperature is also rapid, as demonstrated by a functional recovery experiment in which the foam is submerged in body temperature water (ESI†). Large volume expansions suit this SMP foam well for space-filling applications where large volume expansions are desired.

In summary, we have employed a modified porogen-leaching technique to fabricate PCL-*co*-PEG scaffolds with shape memory capability. We have shown that recovery at body temperature can be achieved through control of the composition of the scaffolds. This may also be achieved through control of the deformation temperature during programming. In addition, we have shown that these scaffolds possess two-way reversible shape actuation. More generally, SMP foams may serve as functional tissue engineering constructs that can be delivered minimal invasively, due to high compression ratios and stable temporary shapes, and as platforms to study cell mechanobiology in active 3D environments, where shape change under cytocompatible conditions is required.

This work was supported by DARPA Young Faculty Award no. D12AP00271 to JHH. Dr Taekwoong Chung is acknowledged for preliminary studies on similar materials under the advisement of PTM. We thank Sanjay Dialani for his work with implementing the salt fusion technique. The content of the present study does not necessarily reflect the position or the policy of the Government, and no endorsement should be inferred.

Notes and references

1 V. P. Shastri, *Artif. Organs*, 2006, **30**, 828–834.
2 G. Chan and D. J. Mooney, *Trends Biotechnol.*, 2008, **26**, 382–392.
3 J. M. Karp and R. Langer, *Curr. Opin. Biotechnol.*, 2007, **18**, 454–459.
4 C. M. Yakacki and K. Gall, in *Shape-Memory Polymers*, Springer, 2010, pp. 147–175.
5 K. A. Davis, K. A. Burke, P. T. Mather and J. H. Henderson, *Biomaterials*, 2011, **32**, 2285–2293.

6 V. P. Shastri and A. Lendlein, *Adv. Mater.*, 2009, **21**, 3231–3234.
7 D. M. Le, K. Kulangara, A. F. Adler, K. W. Leong and V. S. Ashby, *Adv. Mater.*, 2011, **23**, 3278–3283.
8 S. Neuss, I. Blomenkamp, R. Stainforth, D. Boltersdorf, M. Jansen, N. Butz, A. Perez-Bouza and R. Knuechel, *Biomaterials*, 2009, **30**, 1697–1705.
9 J. Cui, K. Kratz, M. Heuchel, B. Hiebl and A. Lendlein, *Polym. Adv. Technol.*, 2011, **22**, 180–189.
10 L.-F. Tseng, P. T. Mather and J. H. Henderson, *Acta Biomater.*, 2013, DOI: 10.1016/j.actbio.2013.06.043.
11 P. T. Knight, K. M. Lee, T. Chung and P. T. Mather, *Macromolecules*, 2009, **42**, 6596–6605.
12 K. M. Lee, P. T. Knight, T. Chung and P. T. Mather, *Macromolecules*, 2008, **41**, 4730–4738.
13 D. Zhang, K. M. Petersen and M. A. Grunlan, *ACS Appl. Mater. Interfaces*, 2012, **5**, 186–191.
14 W. L. Murphy, R. G. Dennis, J. L. Kileny and D. J. Mooney, *Tissue Eng.*, 2002, **8**, 43–52.
15 T. Sauter, K. Kratz and A. Lendlein, *Macromol. Chem. Phys.*, 2013, **214**, 1184–1188.
16 A. A. Lee, T. Delhaas, A. D. McCulloch and F. J. Villarreal, *J. Mol. Cell. Cardiol.*, 1999, **31**, 1833–1843.
17 P. Singhal, J. N. Rodriguez, W. Small, S. Eagleston, J. Van de Water, D. J. Maitland and T. S. Wilson, *J. Polym. Sci., Part B: Polym. Phys.*, 2012, **50**, 724–737.
18 X. Liu and P. X. Ma, *Ann. Biomed. Eng.*, 2004, **32**, 477–486.
19 C. M. Murphy, M. G. Haugh and F. J. O'Brien, *Biomaterials*, 2010, **31**, 461–466.
20 J. Zeltinger, J. K. Sherwood, D. A. Graham, R. Müeller and L. G. Griffith, *Tissue Eng.*, 2001, **7**, 557–572.
21 X. Xu, K. A. Davis, P. Yang, X. Gu, J. H. Henderson and P. T. Mather, *Macromol. Symp.*, 2011, **309**, 162–172.
22 E. D. Rodriguez, X. Luo and P. T. Mather, *ACS Appl. Mater. Interfaces*, 2011, **3**, 152–161.
23 X. Gu and P. T. Mather, *Polymer*, 2012, **53**, 5924–5934.
24 T. Xie, K. A. Page and S. A. Eastman, *Adv. Funct. Mater.*, 2011, **21**, 2057–2066.
25 C. M. Yakacki, R. Shandas, C. Lanning, B. Rech, A. Eckstein and K. Gall, *Biomaterials*, 2007, **28**, 2255–2263.
26 K. Kratz, S. A. Madbouly, W. Wagermaier and A. Lendlein, *Adv. Mater.*, 2011, **23**, 4058–4062.
27 H. X. Zhu and A. H. Windle, *Acta Mater.*, 2002, **50**, 1041–1052.
28 T. Chung, A. Romo-Uribe and P. T. Mather, *Macromolecules*, 2008, **41**, 184–192.
29 J. Li, W. R. Rodgers and T. Xie, *Polymer*, 2011, **52**, 5320–5325.
30 H. Qin and P. T. Mather, *Macromolecules*, 2008, **42**, 273–280.
31 J. Zotzmann, M. Behl, D. Hofmann and A. Lendlein, *Adv. Mater.*, 2010, **22**, 3424–3429.
32 B. J. De Blonk and D. C. Lagoudas, *Smart Mater. Struct.*, 1998, **7**, 771–783.
33 A. Metcalfe, A. C. Desfaits, I. Salazkin, L. Yahia, W. M. Sokolowski and J. Raymond, *Biomaterials*, 2003, **24**, 491–497.
34 D. J. Maitland, W. Small, J. M. Ortega, P. R. Buckley, J. Rodriguez, J. Hartman and T. S. Wilson, *J. Biomed. Opt.*, 2007, **12**, 030504.
35 P. Singhal, A. Boyle, M. L. Brooks, S. Infanger, S. Letts, W. Small, D. J. Maitland and T. S. Wilson, *Macromol. Chem. Phys.*, 2013, **214**, 1204–1214.
36 D. J. Maitland, M. F. Metzger, D. Schumann, A. Lee and T. S. Wilson, *Lasers Surg. Med.*, 2002, **30**, 1–11.
37 H. M. Wache, D. J. Tartakowska, A. Hentrich and M. H. Wagner, *J. Mater. Sci.: Mater. Med.*, 2003, **14**, 109–112.

